Potent antitumor actions of the new antibiotic boningmycin through induction of apoptosis and cellular senescence

Ning Gao, Boyang Shang, Xiumin Zhang, Cong Shen, Rong Xu, Hongzhang Xu, Ruxian Chen and Qiyang He

Boningmycin, a new antibiotic of the bleomycin family, is isolated from the fermentation broth of *Streptomyces verticillus* var. pingyangensis n.sp. This study aimed to evaluate its antitumor actions and mechanism. The results showed that boningmycin exhibited potent inhibitory effects on several human solid tumor cells and that it was stronger than bleomycin. The administration of boningmycin inhibited the growth of human hepatoma HepG2 xenografts in nude mice, with more efficacy than that of bleomycin. Boningmycin led to an increase of the reactive oxygen species involving iron and caused G_2/M phase accumulation in the HepG2 and human breast cancer MCF-7 cells. Two types of cell death, apoptosis and senescence, were detected after exposure to boningmycin. The accumulation of sub-G_1 phase cells, an index of apoptosis, and the activation of caspase apoptotic pathways were detected after treatment with higher concentrations of boningmycin. Low concentrations of boningmycin led to a senescent phenotype with an increase in senescence-associated β-galactosidase activity and the time-dependent increase of p21, p27, and p53 expressions from 48 to120 h. Taken together, the results showed that boningmycin exhibits potent antitumor actions through the induction of apoptosis and cellular senescence. *Anti-Cancer Drugs* 22:166–175 © 2011 Wolters Kluwer Health | Lippincott Williams & Wilkins.

Anti-Cancer Drugs 2011, **22**:166–175

Keywords: antitumor action, apoptosis, bleomycin family, boningmycin, senescence

Institute of Medicinal Biotechnology, Peking Union Medical College and Chinese Academy of Medical Sciences, Beijing, People's Republic of China

Correspondence to Qiyang He, PhD, or Ruxian Chen, PhD, Institute of Medicinal Biotechnology, Peking Union Medical College and Chinese Academy of Medical Sciences, Beijing 100050, PR China
Tel: +86 10 63131856; fax: +86 10 63017302;
e-mail: qyh2000bj@yahoo.com.cn, chrx888@sohu.com

Received 27 April 2010 **Revised form accepted** 16 September 2010

Introduction

The antitumor antibiotic bleomycin (BLM) has long been used in first-line clinical cancer chemotherapy for several malignant tumors, including squamous cell carcinoma, malignant lymphoma, testicular cancer, ovarian cancer, and in combination with other antitumor agents. The advantages of BLM are that it does not damage bone marrow cells or suppress immune functions. However, its main side effect of inducing pulmonary fibrosis retards further application in the clinic [1,2]. Attempts have been made to develop new superior BLM derivatives to improve the antitumor activity and overcome the drawbacks of severe pulmonary toxicity.

A new antibiotic, boningmycin (BON), a member of the BLM family, was isolated from the fermentation broth of *Streptomyces verticillus* var. pingyangensis n.sp [3]. The clinically used form of BLM contains a mixture of BLM A and B. In contrast, BON has a single chemical structure with a different terminal amine moiety (Fig. 1). It shows some antibacterial activity and a stronger antitumor activity toward several human tumor cell lines. However, it remains unknown how BON inhibits tumor cells.

Accumulating evidence shows that the induction of apoptosis plays a very important role in tumor chemotherapy [4,5]. Both extrinsic and intrinsic apoptotic signaling pathways are triggered by various antitumor agents. The extrinsic pathway is mediated by the engagement of death receptors on the cell membrane. The formation of the death-induced signaling complex recruits caspase-8 and promotes the cascade of procaspase activation that follows. The intrinsic pathway initiates the apoptotic cascades by the convergence of signaling at the mitochondria and then follows the alteration of the mitochondrial membrane potentials, the release of cytochrome c into the cytosol, and the activation of the caspase cascade [6,7]. In addition to apoptosis, most tumor cells retain the ability to sustain permanent growth arrest or undergo nonapoptotic types of cell death, such as necrosis, autophagy, senescence, and mitotic catastrophe [8,9]. Initiation of the senescent program determined the outcome of chemotherapy in the mice model [10]. The senescent phenotypes including the enlargement of cell volume and flat shape with elevation of senescence-associated β galactosidase (SA β-gal) appear after exposure to several antitumor agents, especially DNA-damaged agents such as doxorubicin, lidamycin, and BLM [11–13].

Earlier studies showed that the induction of apoptosis by BLM is accomplished by the mitochondria-mediated apoptotic pathway (intrinsic), without involving the Fas receptor-mediated apoptotic pathway [14–17]. The

0959-4973 © 2011 Wolters Kluwer Health | Lippincott Williams & Wilkins DOI: 10.1097/CAD.0b013e3283409bee

Fig. 1

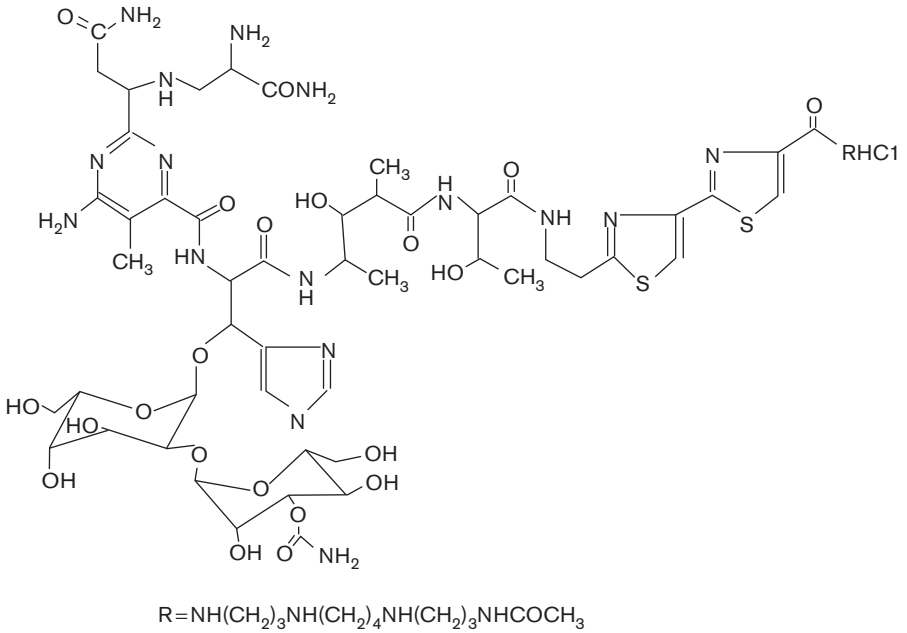

$R=NH(CH_2)_3NH(CH_2)_4NH(CH_2)_3NHCOCH_3$

Chemical structure of boningmycin.

mechanism of its action is mediated by the generation of reactive oxygen species (ROS), degraded DNA and RNA in a selective manner and then arrest of tumor cells at the G_2/M phase [18–22].

In this study, we aimed to investigate the mechanisms of antitumor action of BON *in vitro* and *in vivo*. The results show that it has a higher efficacy than that of BLM. Activation of the apoptotic caspase pathway and the induction of senescence contribute to its action on tumor cells. BON is a promising potential antitumor agent for further drug development.

Methods

Drugs and chemicals

BON was extracted from the fermentation broth of *S. verticillus* var. pingyangensis n.sp and purified according to the method reported earlier [3]. The purity was more than 90% by the examination of high performance liquid chromatography. It was prepared into a 2 μmol/l solution with PBS buffer and stored at −20°C before use. BLM was purchased from Nippon Kayaku (Tokyo, Japan) and dissolved in PBS at 10 mg/ml. Dimethyl sulfoxide, 3-(4,5-dimethyl-2-thiazoyl)-2,5-diphenyl-2H-tetrazolium bromide (MTT), X-gal, propidium iodide, and deferoxamine (DFO) were purchased from Sigma–Aldrich Chemical Inc. (St Louis, Missouri, USA). H_2DFFDA, RPMI 1640, and Dulbecco's modified Eagle's medium were obtained from Invitrogen (Carlsbad, California, USA).

Cell lines and cell culture

Human hepatoma HepG2 cells, breast cancer MCF-7 cells, and aryngocarcinoma KB cells were purchased from the American Type Culture Collection. Human colon carcinoma HCT-116 p53 wild-type (+/+) and p53 knocked-out (−/−) cells were a gift from Dr Bert Vogelstein (Johns Hopkins University, Baltimore, USA). The cell lines were cultured in RPMI 1640 or Dulbecco's modified Eagle's medium medium supplemented with 10% fetal bovine serum, 100 units/ml penicillin, and 100 μg/ml streptomycin. All cultures were maintained in an incubator at 37°C with 5% CO_2 in a humidified atmosphere.

Cytotoxicity assays

Cell viability was assessed using the MTT assay. The cells were seeded into a 96-well plate at a cell density of 4000 per well for 24 h, followed by drug treatment for 72 h. Next, 5 μl of 5 mg/ml MTT was added to the medium and incubated for 2 h at 37°C. After removing the culture medium, 200 μl of dimethyl sulfoxide was added. The plates were read using an enzyme-linked immunosorbent assay plate reader at 570 nm. The viability of untreated cells was set as 100% and the viability in other groups was calculated by comparing the optical density reading with the control. IC_{50} value was calculated from the nonlinear regression analysis.

Cell cycle analysis

The cells were trypsinized and washed once with PBS, and then fixed with cold 70% ethanol overnight. The

fixed cells were washed twice with PBS and incubated with 100 μg/ml of ribonuclease A at 37°C for 30 min and then stained in PBS containing 50 μg/ml propidium iodide for 1 h. The fluorescence intensity was detected using BD FACSCalibur cytometer (BD Biosciences, California, USA) and the cell cycle distribution was assayed using the ModFit LT software (BD Biosciences).

Measurement of reactive oxygen species

After treatment with 2 μmol/l BON at different timepoints, the cells were stained with 5 μmol/l H_2DFFDA, ROS-specific dye, for 1 h at 37°C. The cells were harvested and then immediately underwent flow cytometric analysis with excitation and emission settings of 488 nm and 530 nm, respectively. For each sample, 10 000 cells were counted.

Detection of senescence-associated β-galactosidase activity

SA β-gal staining was performed according to the method described earlier [12]. The fixed cells were incubated in a fresh X-gal staining solution containing 40 mmol/l sodium citrate (pH 6.0), 150 mmol/l sodium chloride, 5 mmol/l potassium ferricyanide, 5 mmol/l of potassium ferrocyanide, 2 mmol/l magnesium chloride, and 1 mg/ml of 5-bromo-4-chloro-3-indoyl b-D galactoside (X-gal) for 12–16 h at 37°C. The number of SA β-gal-positive cells was scored with a total of 300 cells.

Western blot analysis

Cells were lysed with the lysis buffer containing 50 mmol/l Tris–HCl (pH 7.5), 250 mmol/l NaCl, 5 mmol/l EDTA, 50 mmol/l NaF, 1 mmol/l DTT, 1% Triton X-100, 1 mmol/l sodium orthovanadate, and protease inhibitors. After centrifugation, the supernatant fraction was removed and protein concentrations were determined using the Bio-Rad protein assay. Proteins were resolved by SDS-PAGE and transferred onto a polyvinylidene fluoride membrane. After blocking with 5% nonfat milk in the blocking buffer (PBS containing 0.1% Tween 20, pH 7.5), the membrane was incubated with the desired primary antibody for 2 h at room temperature and then incubated with an appropriate peroxidase-conjugated secondary antibody. The immunoreactive bands were visualized using the ECL Plus Western Blotting Detection System (Piscataway, New Jersey, USA). The level of β-actin for each sample was used as a loading control. The antibodies against cleaved caspase-3, caspase-7, caspase-8, caspase-9, and cleaved/total polymerase [poly(ADP-ribose) polymerase (PARP)] were from Cell Signaling Technology, Inc. (Danvers, Massachusetts, USA). The antibodies against p53, p27, p21, and actin were from Santa Cruz Biotechnology, Inc. (Santa Cruz, California, USA).

Small interfering RNA interference

HepG2 cells were transfected with Lipofectamine 2000 (Invitrogen) according to the manufacturer's instructions using one double-stranded small interfering RNA (siRNA) oligonucleotides per gene (100 pmol of each siRNA). Cell treatments were started 24 h after plating. p21 siRNA: 5′-GACCAUGUGGACCUGUCAC-3′, p27 siRNA: 5′-GCACUGCAGAGACAUGGA A-3′.

Reverse transcriptase-PCR

RNA (500 ng) was reverse-transcribed with the Moloney murine leukemia virus reverse transcriptase (Promega Corporation, Madison, Wisconsin, USA) and oligo d(T) 16 primer (Promega) in 20 μl of reaction mixture. The resulting cDNA (1–2 μl) was amplified by PCR for Fas and glyceraldehyde-3-phosphate dehydrogenase. cDNA was amplified in 28–32 cycles, consisting of denaturing for 30 s at 94°C, annealing for 45 s at 52°C or 50°C, and primer extension for 30 s at 72°C. Fas forward primer: CCAAGTG ACTGACATCAACTC and reverse primer: CTCTTTGCA CTTGGTGTTGCTGG, glyceraldehyde-3-phosphate dehydrogenase forward primer: CGGAGTCAACGGATTTG GTCGTAT and reverse primer: AGCCTTCTCCATGG TGGTGAAGAC were used for reverse transcriptase-PCR.

Animal experiments

The nude mice with a BALB/c genetic background (female, ages 4–6 weeks, 18–20 g in weight) were obtained from the Institute of Experimental Animals, Chinese Academy of Medical Sciences. Animal care was in compliance with the regulation issued by the Beijing Committee of Laboratory Animals. All experiments were carried out under specific pathogen-free conditions using laminar airflow racks. All food and water was sterilized and provided *ad libitum*. Before beginning the experiment, the mice were allowed to acclimatize for a week.

The inhibitory effect of BON on human hepatoma HepG2 xenografts was examined in nude mice with a BALB/c genetic background. Under sterile conditions, well-developed tumors were cut into 1-mm^3 fragments and transplanted subcutaneously into the right flank of nude mice using a trocar. When the tumor reached a volume between 100 and 200 mm^3, the mice were randomly assigned into control and treatment groups. Control groups were given saline alone, and treatment groups were administrated with BLM or BON (intraperitoneally). The sizes of the tumors were measured twice every 3 days using microcalipers. The tumor volume (V) was calculated as follows: $V = (\text{length} \times \text{width}^2)/2$. On day 15 after drug administration, mice were killed, and tumors were removed and weighed. The ratio of tumor growth inhibition was calculated by the formula: $(A–B)/A \times 100\%$ (where A is the average tumor weight of the control group, and B is the average tumor weight of the experimental group).

Statistical analysis

Data were expressed as means with standard deviations. SAS6.12 software (SAS Ltd., North Carolina, USA) was used for statistical analysis. Student's t-test was applied for comparison of the means of two groups, and analysis

of variance was used for the means of multiple groups. For all of the value differences, P value less than 0.05 was considered significant.

Results

The potent cytotoxicity of boningmycin on human tumor cells

The growth-inhibitory effects of BON on six types of human tumor cell lines were examined by the MTT assay. A variation in the sensitivity to BON was observed among the cell lines with an IC_{50} ranging from 0.47 to 3.07 μmol/l, showing more potent cytotoxicity than that of BLM (Table 1). The similar susceptibility to BON appeared between HCT-116 p53 + / + and p53 – / – cells, suggesting that the action of BON is not dependent on the function of the p53 protein. The hepatoma HepG2 and MCF-7 cells were selected for further studies as the Chinese population has a high incidence of hepatoma and it requires new antitumor agents for clinical usefulness.

Potent antitumor activity of boningmycin *in vivo*

To evaluate its potential use as an antineoplastic agent against hepatoma, BON was administered to the human hepatoma HepG2 xenograft nude mice. The intraperitoneally administration of the drugs, every 3 days, started when the HepG2 tumor size in the nude mice was between 150 and 200 mm^3. The significant suppression of HepG2 tumor growth in a dose-dependent manner was shown by observing the tumor size and weight. On day 15, the groups treated with 1 and 9 mg/kg of BON significantly caused a dose-dependent suppression of tumor growth in this tumor model (Fig. 2a). The inhibitory percentages of tumor growth were 43.9% and 72.2% after the administration of 1 mg/kg and 9 mg/kg BON, respectively (Fig. 2b). BLM also showed evident antitumor efficiency in this model, although when given at the same dosage (9 mg/kg) and with the same schedule, BON was more potent than BLM. No toxicity was observed during the whole experimental period (data not shown).

Arrest of the cells at the G_2/M phase by boningmycin

The cell cycle distribution was assayed by flow cytometry after the HepG2 and MCF-7 cells were treated with the drugs for 24 h. As the BON concentration increased from 0 to 2 μmol/l, the proportion of the HepG2 G_2/M phase cells and the MCF-7 cells increased from 12.4% to 81.2% and 12.3% to 81.3%, respectively (Fig. 3). It is consistent with BLM action on MCF-7 cells, although at the same concentration, BON was more potent than BLM (Fig. 3a).

Table 1 Cytotoxicities of BON and BLM on human solid tumor cell lines

Cell lines	BON (IC_{50}/μmol/l)	BLM (IC_{50}/μmol/l)
HepG2	0.72 ± 0.20	1.70 ± 0.18
MCF-7	0.68 ± 0.16	1.12 ± 0.22
A549	1.01 ± 0.04	1.82 ± 0.11
HeLa	3.07 ± 0.31	4.01 ± 0.29
KB	0.94 ± 0.08	2.01 ± 0.26
HCT116 (p53 wild type)	0.47 ± 0.04	0.69 ± 0.12
HCT116 (p53 knocked out)	0.50 ± 0.16	1.20 ± 0.10

The cells were treated with various concentrations of BON and BLM for 72 h. Cell survival was determined by the 3-(4,5-dimethyl-2-thiazoyl)-2,5-diphenyl-2H-tetrazolium bromide assay. The data represents the mean ± standard deviation from three independent experiments.
BLM, bleomycin; BON, boningmycin.

Fig. 2

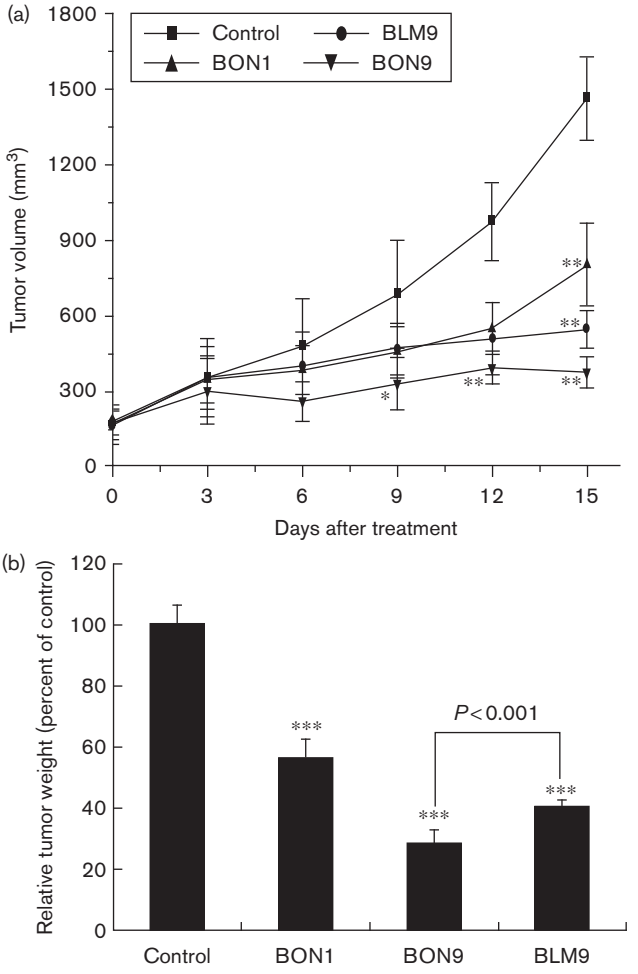

Inhibition of human hepatoma HepG2 tumor growth by boningmycin (BON) and bleomycin (BLM) in nude mice. The tumor-bearing nude mice were intraperitoneally administered five times every 3 days with BLM or BON, whereas the control group was administered with saline. On day 15 after tumor cell inoculation, the mice were killed and the tumors were removed and weighed. (a) Change in tumor volume after administration with BON and BLM; (b) the percentages of tumor weight (control 100%) were shown on the last day of the subject experiment.

Generation of ROS triggered by boningmycin with the involvement of iron

To assess the involvement of free radicals in the BON-mediated cell death, the specific fluorescent dye H_2DFFDA was used to monitor the generation of ROS. HepG2 cells were treated with 2 μmol/l of BON for 4, 12, and 24 h. Increase of ROS was detected at 4 h, and

Fig. 3

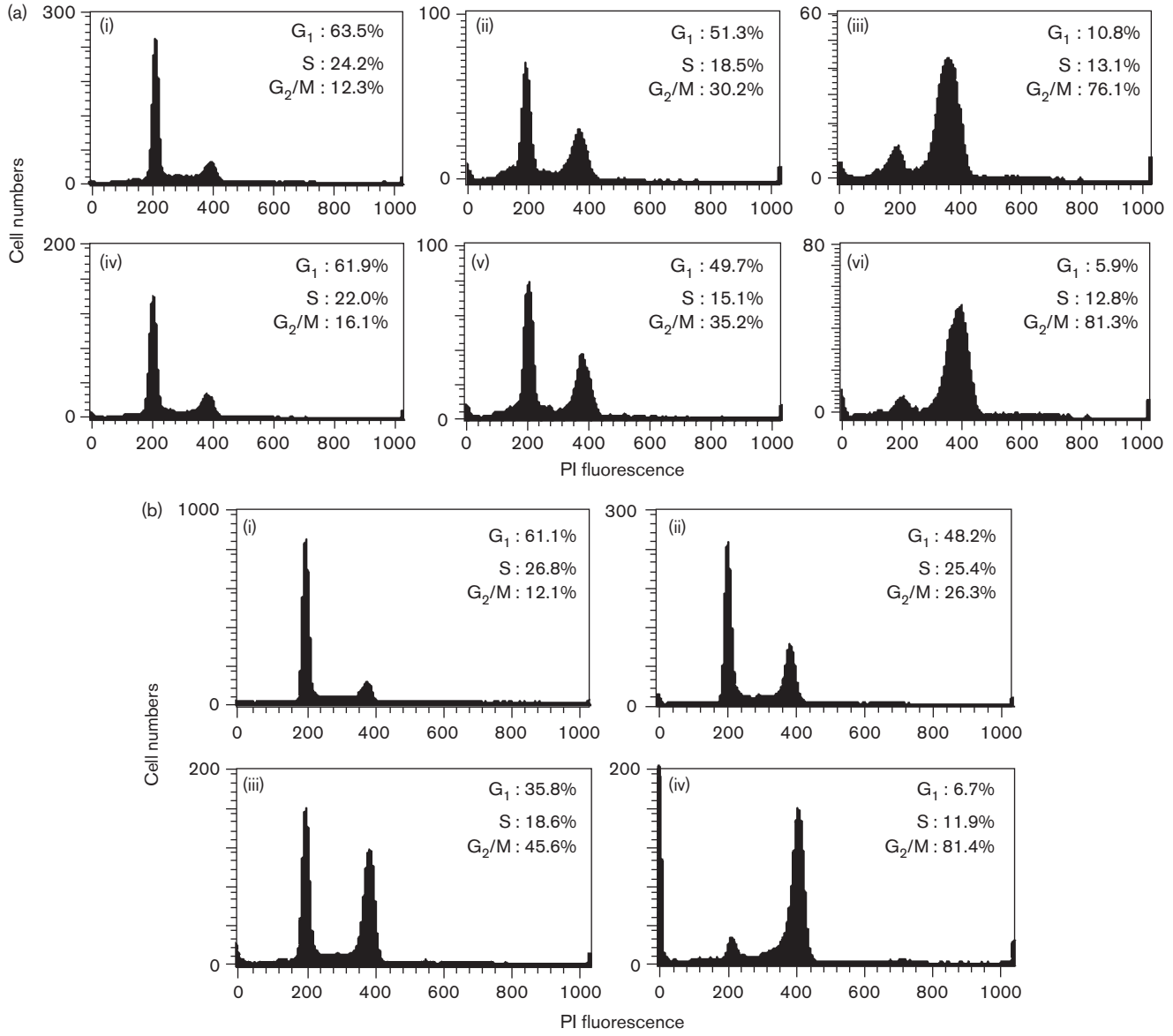

Arrest of the cell cycle at the G_2/M phase by boningmycin (BON) and bleomycin (BLM) in HepG2 and MCF-7 cells. The fixed cells were stained with propidium iodide (PI) and detected by flow cytometry. (a) The MCF-7cells were treated with the drugs for 24 h: (i) control; (ii) 0.5 μmol/l BLM; (iii) 2 μmol/l BLM; (iv) 0.1 μmol/l BON; (v) 0.5 μmol/l BON; (vi) 2 μmol/l BON. (b) The HepG2 cells were treated with BON for 24 h: (i) control; (ii) 0.1 μmol/l; (iii) 0.5 μmol/l; (iv) 2 μmol/l BON. The results are representative of three independent experiments.

reached 180% at 24 h (Fig. 4a–d). To confirm whether the process of BON action involved iron ions, the cells was exposed to 10 μmol/l DFO, a chelator of iron, for 24 h. The generation of ROS by BON was terminated after treatment with DFO (Fig. 4f), suggesting that iron is required for the BON action, as does BLM.

Induction of caspase-dependent apoptosis by boningmycin

To test whether BON induced apoptosis, a DNA content analysis was used, as the sub-G_1 content of DNA is typically indicative of apoptosis. The data showed a concentration-dependent increase of the sub-G1 phase from 14.6 to 35.0%, after the HepG2 cells were exposed to different concentrations of BON (0.2, 1, 2 μmol/l) for 48 h (Fig. 5a). However, apoptotic cells were rarely detected after the treatment with BON only for 24 h (data not shown).

The activation of the caspase pathway initiated by BON was analyzed with western blot in the HepG2 cells (Fig. 5b). The PARP cleavage, an indicative marker of apoptosis, was markedly observed after exposure to high

Fig. 4

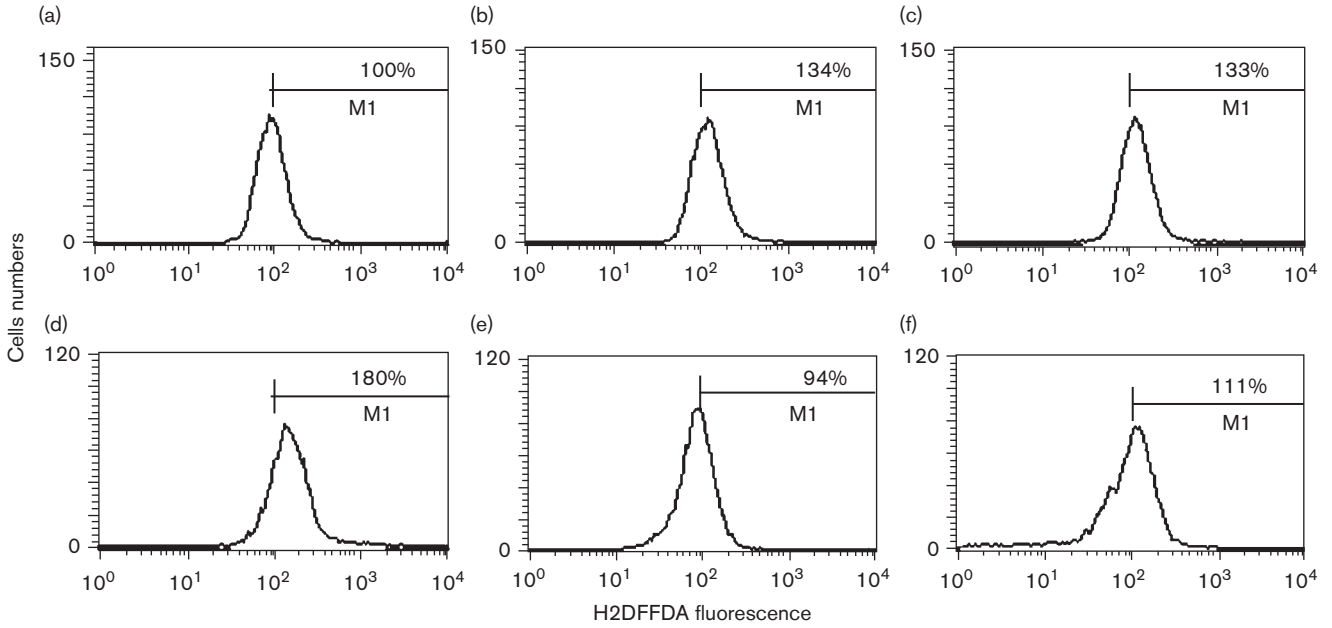

The generation of reactive oxygen species triggered by boningmycin (BON) with the involvement of iron in the HepG2 cells. After staining with 5 μmol/l of H_2DFFDA in fresh medium for 1 h, the cells were assayed using a FACSCalibur cytometer. The cells were incubated with 2 μmol/l BON for 4 h (b), 12 h (c), and 24 h (d and f) and 10 μmol/l of deferoxamine alone (e), or plus BON (f) for 24 h, respectively. (a) represents the drug-untreated cells. The results are representative of three independent experiments.

concentrations of BON for 48 h and it also caused a time-dependent upregulation of the p53 protein from 12 h onwards. The cleavages of caspase-3, caspase-7, caspase-8, and caspase-9 were detected from 8 to 48 h, suggesting the apoptotic pathway was activated by BON and mainly involved the intrinsic apoptotic pathway. To clarify whether the extrinsic apoptotic pathway also played a role, we used the siRNA interference to knockdown the Fas expression in the HepG2 cells. Three pairs of siRNA oligos were designed complementary to the human Fas mRNA. After the transfection of HepG2 cells for 48 h, a significant reduction of the Fas mRNA was observed by reverse transcriptase-PCR with Fas1 and Fas3 siRNA (Fig. 5c). However, a similar level of PARP cleavage was detected in the Fas-knockeddown cells after exposure to 2 μmol/l BON for 48 h (Fig. 5d). Thus, it is the intrinsic apoptosis pathway that plays a key role in the BON-induced apoptosis.

Induction of senescence by low concentrations of boningmycin

Induction of senescence by BLM had been reported and it might be predictive for the same role of BON. When HepG2 and MCF-7 cells were treated with low concentrations of BON for 120 h, they showed a phenotype that is typical of cellular senescence: a distinct, flat, and enlarged morphology, and irreversible growth inhibition with elevation of SA β-gal activity (Fig. 6a). Quantitative analyses for cellular senescence showed that the percentage of the cells with SA β-gal staining increased in a concentration-dependent manner (Fig. 6b and c).

The molecular features of the senescent cells elicited by BON were analyzed. The time-dependent increase of p21 and p27 expression, two cyclin-dependent kinase inhibitors, was detected after the treatment of HepG2 cells with BON from 48 to120 h and the expression of the p53 protein was transiently increased in the BON-induced senescent cells (Fig. 7a). To discern the difference between senescence and apoptosis, PARP cleavage and full length of caspase-3 were analyzed. A small portion of the cleavage fragment of PARP appeared from 48 to 120 h after exposure to BON, suggesting that it is distinct from apoptosis.

It is possible that the upregulation of p21 and p27 expressions helps the cells to evade the BON damage. Silencing of p21 and p27 expressions were performed to clarify this issue. The siRNA oligos were designed complementary to the human p21 and p27 mRNA. Significant reductions of the p21 and/or p27 proteins were confirmed by western blot analysis after the transfection of HepG2 cells with p21, p27, or p21 + p27 siRNA for 48 h (Fig. 7b). The decrease in the cell viability after the silencing of p21 or p27 was detected compared with the mock control after exposure to 0.2, 0.5, and 2 μmol/l of BON for 48 h (Fig. 7c). However, no significant BON cytotoxicities were observed among the p21, p27, or p21 + p27 groups

Fig. 5

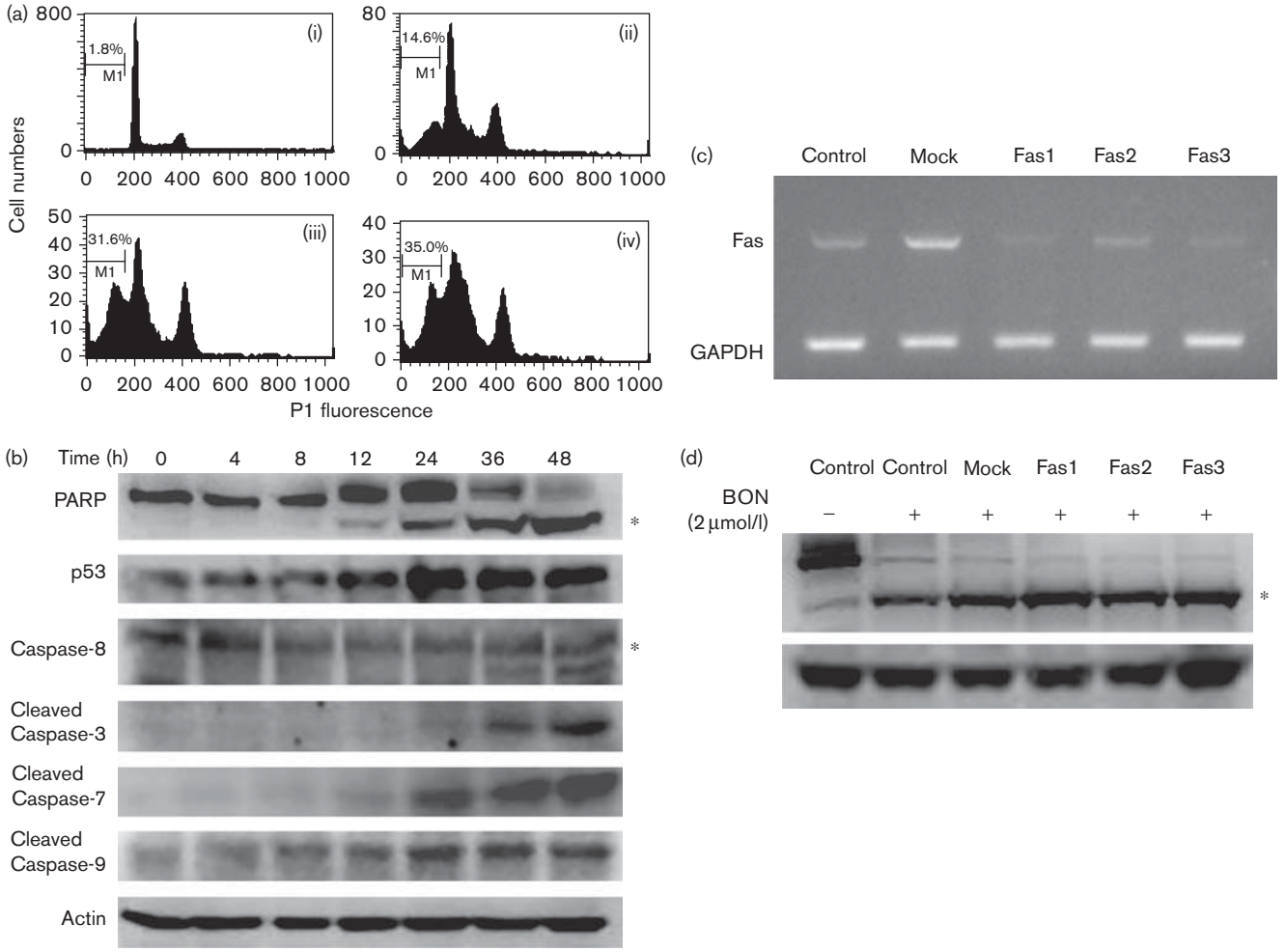

Induction of apoptosis by boningmycin (BON) in the HepG2 cells. (a) Flow cytometric analysis of apoptotic cells. The cells were treated with BON 0 (i), 0.2 μmol/l (ii), 0.5 μmol/l (iii), 1 μmol/l (iv) for 48 h. The harvested cells were stained with propidium iodide (PI) and then the 'sub-G_1' apoptotic cells were detected using a Flow cytometer. (b) Activation of the caspase cascade in BON-induced apoptosis. The HepG2 cells were treated with 2 μmol/l BON for the indicated timepoints. Protein lysates were analyzed by western blot. (c) Reverse transcriptase-PCR results showed the knockdown Fas mRNA level by Fas small interfering RNA transfection. (d) The cleavage of poly(ADP-ribose) polymerase (PARP) is not affected by the knockdown of Fas expression. In (b and d), the asterisk represents a cleavage fragment. The results are representative of two independent experiments. GAPDH, glyceraldehyde-3-phosphate dehydrogenase.

after treatment with different concentrations of BON. The data showed that the increase of the p21 and p27 expression helps the senescent cells survive in the BON damage.

Discussion

In this study, the data showed that the potent inhibitory effects of the new antibiotic BON on tumor were observed *in vitro* and *in vivo*, and its efficacy is stronger than that of BLM, a kind of a normally clinically used antitumor agent. The mechanism of antitumor action of BON is mediated by the induction of apoptosis and senescence. Our earlier results showed that BON exerts the lowest pulmonary toxicity among the BLM members (data not shown). It can be concluded that BON is a very promising antibiotic as a candidate drug for the chemotherapy of human malignancies and deserves further investigation.

It is well known that the action of BLM on tumor cells includes: (i) binding with iron after entering the cells, (ii) damaging DNA and RNA, (iii) determining cell fate response to the damage [1,2]. According to the data presented here, the action of BON is similar to that of BLM. The damage signals triggered by BLM led to the following response: generation of ROS and arrest of cell cycle, finally leading to the initiation of the cell death program, such as apoptosis and senescence. Our data showed that intracellular ROS was accumulated and the caspase-dependent pathways were activated during the process of BON-induced apoptosis, suggesting that it is mediated by the mitochondrial apoptotic pathway.

Fig. 6

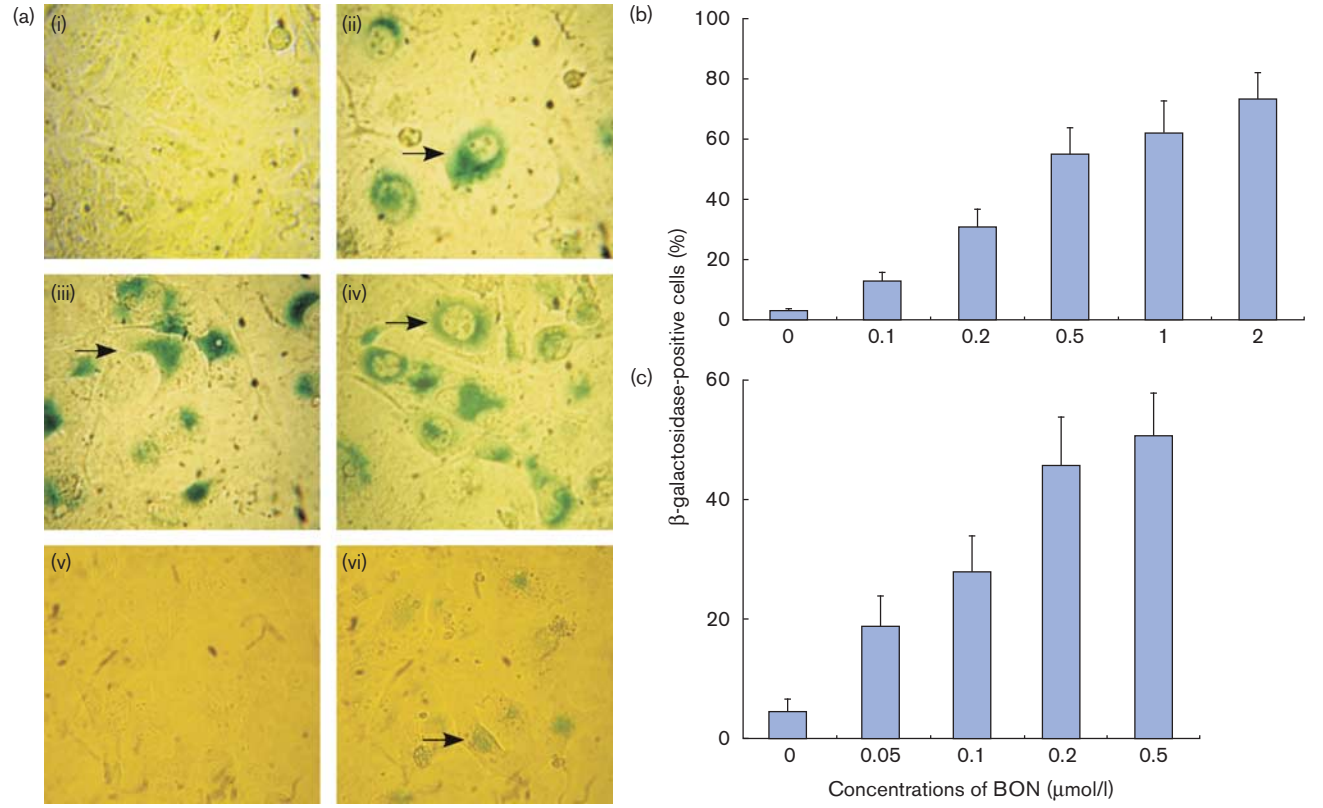

Senescence phenotypes induced by boningmycin (BON). (a) The MCF-7 cells were incubated with 0.1 μmol/l (ii), 0.5 μmol/l (iii) and 2 μmol/l (iv) BON and the HepG2 cells were incubated with 0.1 μmol/l BON(vi) for 3 days. (i) and (v) represent the drug-untreated cells. (b) The percentages of β-galactosidase-positive cells in the HepG2 cells. (c) The percentages of β-galactosidase-positive cells in the MCF-7 cells. The results are representative of three independent experiments.

Although the cleavage of caspase-8 was detected in the BON-treated cells (Fig. 5), it seems that it did not involve the extrinsic apoptotic pathways, as several reports elucidated that the indirect increase of Fas expression was observed in BLM-induced apoptosis [11,12].

Senescence has been viewed primarily as a property of normal cells, which is lost during neoplastic transformation and it plays an important role in the inhibition of tumors [23–26]. The results of this study indicate that in the presence of low BON concentration, the cells apparently showed all the morphological and biochemical changes associated with senescence, consistent with the effects of BLM on normal cells and tumor cells [13,27,28]. The molecular features of BON-induced senescence are the elevation of p21 and p27 expressions, by which the senescent cells were permanently retarded at the G_2/M phase. The activation of p21 expression is a feature of senescent cells [29,30]. Recently, the inactivation of Skp2, regulator of the p27 protein, led to tumor senescence [31]. The transient increase of the p53 protein elicited by BON is consistent with that of BLM in normal fibroblast NHF3 and MRC5 cells [13]. The phenomena were also observed in hydrogen peroxide-induced senescence [32]. It differs in apoptosis in which p53 expression increases continuously. Although apoptosis and senescence are distinct programs initiated by antitumor agents, the final fate of senescent cells is death through caspase-dependent apoptosis in doxorubixin-induced cell death [33]. It is the reason why a few apoptotic cells were detected after exposure to low concentrations of BON for 48 h.

The use of the terms mitotic cell death and senescence is often confused and mixed according to tumor cell response to antitumor agents. Some studies strictly described these phenomena as mitotic cell death with senescent phenotype [11,33]. Two types of cell death, mitotic cell death and apoptosis, were reported after electropermeabilization of BLM into tumor cells, depending on the number of BLM molecules internalized [34,35]. These features were also observed in BON-induced cell death. As a matter of fact, drug-induced senescence in tumor cells is comparable with that in normal cells except the arrest of cells at the G_2/M phase. It seems reasonable to describe them as senescence, considering that it will play an important role in tumorigenesis and chemotherapy for tumor.

Fig. 7

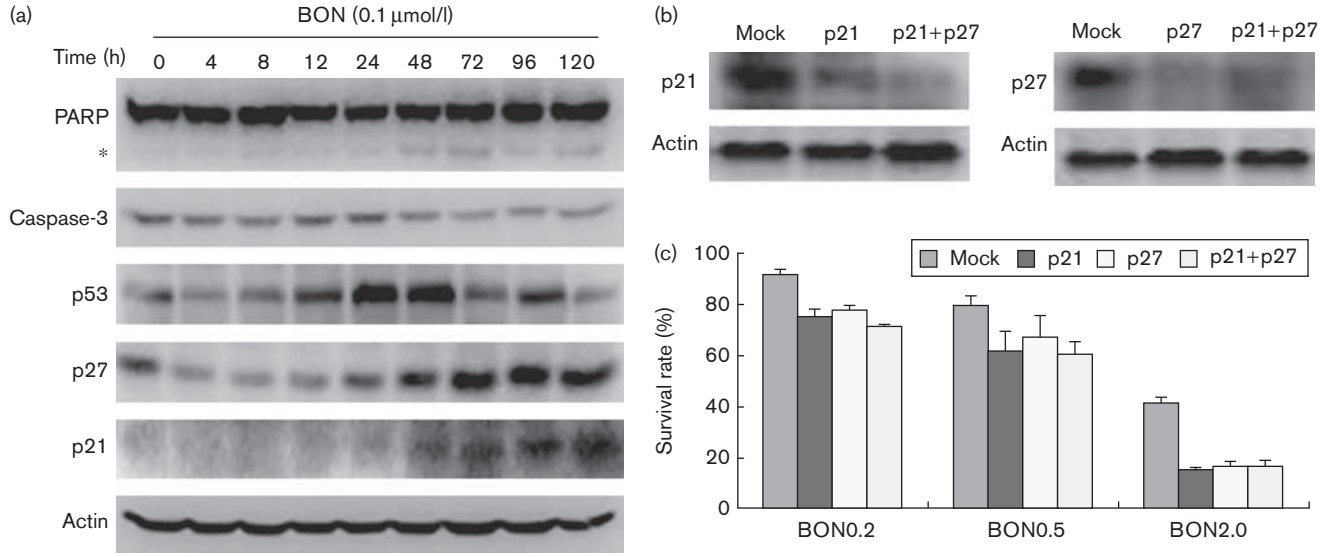

Molecular characteristic protein expressions in the senescent HepG2 cells. (a) The cells were harvested at the indicated timepoints after exposure to 0.1 μmol/l boningmycin (BON) and the expression of senescent-related proteins was detected by western blot. (b) Reduction of p21 and p27 expressions after the small interfering RNA transfection. p21 + p27 represents a double knockdown group. (c) Cell viability after silencing the p21 and p27 expressions with treatment with different concentrations of BON. The experiments are repeated at least twice. PARP, poly(ADP-ribose) polymerase.

Interestingly, BON has potent inhibitory effects on hepatoma *in vivo* and *in vitro*. Human hepatocellular carcinoma is one of the leading causes of cancer-related death worldwide, and more than 80% of liver cancer cases occur in the developing countries. In China, it ranks second in cancer incidence because of the high infection of hepatitis B virus [36,37]. Hepatoma has a long latency but is often diagnosed at the later stages when the tumors are of high grade and progress rapidly with a high likelihood of invasion, leading to a poor prognosis. Therefore, it is valuable to carry out further extensive studies to evaluate the antineoplastic effectiveness of BON against hepatomas. The sensitivity of tumors to BLM is also influenced by BLM hydroxylase (BH) through deamination of BLM into the inactive form. It determines the effective action of BLM on the specific tissue-originated tumors with low activity of BH, such as head and neck carcinoma and Hodgkin's lymphoma [38–40]. In HepG2 cells, the amount of BH detected by western blot analysis was similar to the HeLa cells (data not shown). As the apparent difference of the IC_{50} values between the two cells was observed by the MTT assay (Table 1), it is clear that other factors affect the action of BON on different tumors. Further studies are being carried out in our laboratory to answer why BON exerts potent cytotoxity in hepatoma cells at the molecular level.

In summary, the mechanism of the potent inhibitory effect of BON on tumor is because of the induction of apoptosis and cellular senescence. It is more efficient than that of BLM *in vitro* and *in vivo*. BON is a promising potential antitumor agent for further drug development.

Acknowledgement

The study was supported by Grants from the National S&T Major Special Project on Major New Drug Innovation (2009ZX09301-003) and the National Scientific Foundation of China (30772284).

References

1 Chen J, Stubbe JA. Bleomycins: towards better therapeutics. *Nat Rev Cancer* 2005; **5**:102–112.
2 Lazo JS. Bleomycin. *Cancer Chemother Biol Response Modif* 1999; **18**:39–45.
3 Xu H, Yu L, Zhang X, Wang S. Isolation, purification and structure determination of boningmycin (Z-893). *Chin J Antibiot* 2003; **28**:465–467.
4 Johnstone RW, Ruefli AA, Lowe SW. Apoptosis: a link between cancer genetics and chemotherapy. *Cell* 2002; **108**:153–164.
5 Constantinou C, Papas KA, Constantinou AI. Caspase-independent pathways of programmed cell death: the unraveling of new targets of cancer therapy? *Curr Cancer Drug Targets* 2009; **9**:717–728.
6 Wang X. The expanding role of mitochondria in apoptosis. *Genes Dev* 2001; **15**:2922–2933.
7 Danial NN, Korsmeyer SJ. Cell death: critical control points. *Cell* 2004; **116**:205–219.
8 Okada H, Mak TW. Pathways of apoptotic and non-apoptotic death in tumor cells. *Nat Rev Cancer* 2004; **4**:592–603.
9 Cagnol S, Chambard JC. ERK and cell death: mechanisms of ERK-induced cell death–apoptosis, autophagy and senescence. *FEBS J* 2010; **277**:2–21.
10 Schmitt CA, Fridman JS, Yang M, Lee S, Baranov E, Hoffman RM, Lowe SW. A senescence program controlled by p53 and p16INK4a contributes to the outcome of cancer therapy. *Cell* 2002; **109**:335–346.
11 Chang BD, Broude EV, Dokmanovic M, Zhu H, Ruth A, Xuan Y, *et al.* A senescence-like phenotype distinguishes tumor cells that undergo terminal

proliferation arrest after exposure to anticancer agents. *Cancer Res* 1999; **59**:3761–3767.
12 He QY, Liang YY, Wang DS, Li DD. Characteristics of mitotic cell death induced by enediyne antibiotic lidamycin in human epithelial tumor cells. *Int J Oncol* 2002; **20**:261–266.
13 Robles SJ, Adami GR. Agents that cause DNA double strand breaks lead to p16INK4a enrichment and the premature senescence of normal fibroblasts. *Oncogene* 1998; **16**:1113–1123.
14 Müller M, Strand S, Hug H, Heinemann EM, Walczak H, Hofmann WJ, *et al.* Drug-induced apoptosis in hepatoma cells is mediated by the CD95 (APO-1/Fas) receptor/ligand system and involves activation of wild-type p53. *J Clin Invest* 1997; **99**:403–413.
15 Müller M, Wilder S, Bannasch D, Israeli D, Lehlbach K, Li-Weber M, *et al.* p53 activates the CD95 (APO-1/Fas) gene in response to DNA damage by anticancer drugs. *J Exp Med* 1998; **188**:2033–2045.
16 Gibson AA, Harwood FG, Tillman DM, Houghton JA. Selective sensitization to DNA-damaging agents in a human rhabdomyosarcoma cell line with inducible wild-type p53 overexpression. *Clin Cancer Res* 1998; **4**:145–152.
17 Wallach-Dayan SB, Izbicki G, Cohen PY, Gerstl-Golan R, Fine A, Breuer R. Bleomycin initiates apoptosis of lung epithelial cells by ROS but not by Fas/FasL pathway. *Am J Physiol Lung Cell Mol Physiol* 2006; **290**:L790–L796.
18 Sugiura Y, Suzuki T, Kuwahara J, Tanaka H. On the mechanism of hydrogen peroxide-, superoxide-, and ultraviolet light-induced DNA cleavages of inactive bleomycin-iron (III) complex. *Biochem Biophys Res Commun* 1982; **105**:1151–1158.
19 Steighner RJ, Povirk LF. Bleomycin-induced DNA lesions at mutational hot spots: implications for the mechanism of double-strand cleavage. *Proc Natl Acad Sci U S A* 1990; **87**:8350–8354.
20 Holmes CE, Abraham AT, Hecht SM, Florentz C, Giege R. Fe·bleomycin as a probe of RNA conformation. *Nucleic Acids Res* 1996; **24**:3399–3406.
21 Abraham AT, Lin JJ, Newton DL, Rybak S, Hecht SM. RNA cleavage and inhibition of protein synthesis by bleomycin. *Chem Biol* 2003; **10**:45–52.
22 Baus F, Gire V, Fisher D, Piette J, Dulić V. Permanent cell cycle exit in G2 phase after DNA damage in normal human fibroblasts. *EMBO J* 2003; **22**:3992–4002.
23 Michaloglou C, Vredeveld LC, Soengas MS, Denoyelle C, Kuilman T, Van der Horst CM, *et al.* BRAFE600-associated senescence-like cell cycle arrest of human naevi. *Nature* 2005; **436**:720–724.
24 Braig M, Lee S, Loddenkemper C, Rudolph C, Peters AH, Schlegelberger B, *et al.* Oncogene-induced senescence as an initial barrier in lymphoma development. *Nature* 2005; **436**:660–665.
25 Collado M, Gil J, Efeyan A, Guerra C, Schuhmacher AJ, Barradas M, *et al.* Tumour biology: senescence in premalignant tumours. *Nature* 2005; **436**:642.
26 Xue W, Zender L, Miething C, Dickins RA, Hernando E, Krizhanovsky V, *et al.* Senescence and tumour clearance is triggered by p53 restoration in murine liver carcinomas. *Nature* 2007; **445**:656–660.
27 Aoshiba K, Tsuji T, Nagai A. Bleomycin induces cellular senescence in alveolar epithelial cells. *Eur Respir J* 2003; **22**:4364–4343.
28 Kasper M, Barth K. Bleomycin and its role in inducing apoptosis and senescence in lung cells–modulating effects of caveolin-1. *Curr Cancer Drug Targets* 2009; **9**:341–353.
29 Ben-Porath I, Weinberg RA. The signals and pathways activating cellular senescence. *Int J Biochem Cell Biol* 2005; **37**:961–976.
30 Te Poele RH, Okorokov AL, Jardine L, Cummings J, Joel SP. DNA damage is able to induce senescence in tumor cells in vitro and in vivo. *Cancer Res* 2002; **62**:1876–1883.
31 Lin HK, Chen Z, Wang G, Nardella C, Lee SW, Chan CH, *et al.* Skp2 targeting suppresses tumorigenesis by Arf-p53-independent cellular senescence. *Nature* 2010; **464**:374–379.
32 Chen QM, Bartholomew JC, Campisi J, Acosta M, Reagan JD, Ames BN. Molecular analysis of H2O2-induced senescent-like growth arrest in normal human fibroblasts: p53 and Rb control G1 arrest but not cell replication. *Biochem J* 1998; **332**:43–50.
33 Eom YW, Kim MA, Park SS, Goo MJ, Kwon HJ, Sohn S, *et al.* Two distinct modes of cell death induced by doxorubicin: apoptosis and cell death through mitotic catastrophe accompanied by senescence-like phenotype. *Oncogene* 2005; **24**:4765–4777.
34 Tounekti O, Pron G, Belehradek J Jr, Mir LM. Bleomycin, an apoptosis-mimetic drug that induces two types of cell death depending on the number of molecules internalized. *Cancer Res* 1993; **53**:5462–5469.
35 Tounekti O, Kenani A, Foray N, Orlowski S, Mir LM. The ratio of single- to double-strand DNA breaks and their absolute values determine cell death pathway. *Br J Cancer* 2001; **84**:1272–1279.
36 Bosch FX, Ribes J, Borras J. Epidemiology of primary liver cancer. *Semin Liver Dis* 1999; **19**:271–285.
37 Llovet JM, Bruix J. Hepatitis B virus and hepatocellular carcinoma. *J Hepatol* 2003; **39**:59–63.
38 Sebti SM, Jani JP, Mistry JS, Gorelik E, Lazo JS. Metabolic inactivation: a mechanism of human tumor resistance to bleomycin. *Cancer Res* 1991; **51**:227–232.
39 Ferrando AA, Velasco G, Campo E, Lopez-Otin C. Cloning and expression analysis of human bleomycin hydrolase, a cysteine proteinase involved in chemotherapy resistance. *Cancer Res* 1996; **56**:1746–1750.
40 Schwartz DR, Homanics GE, Hoyt DG, Klein E, Abernethy J, Lazo JS. The neutral cysteine protease bleomycin hydrolase is essential for epidermal integrity and bleomycin resistance. *Proc Natl Acad Sci U S A* 1999; **96**:4680–4685.